

Syntheses, Ground Electronic State, and Crystal and Molecular Structure of the Monomeric Manganese(IV) Porphyrin Complex Dimethoxy(5,10,15,20-tetraphenylporphinato)manganese(IV)

MARK J. CAMENZIND, FREDERICK J. HOLLANDER, and CRAIG L. HILL*

Received April 2, 1982

The complex dimethoxy(5,10,15,20-tetraphenylporphinato)manganese(IV), $\text{Mn}^{\text{IV}}\text{TPP}(\text{OCH}_3)_2$, $\text{Mn}(\text{C}_{44}\text{H}_{28}\text{N}_4)(\text{OCH}_3)_2$, has been synthesized by the oxidation of $\text{Mn}^{\text{III}}\text{TPP}(\text{OAc})$ in basic methanol using either sodium hypochlorite or iodosylbenzene as oxidants. The crystal and molecular structure has been determined by X-ray crystallographic methods. The compound crystallized as a partial methanol solvate, $\text{Mn}^{\text{IV}}\text{TPP}(\text{OCH}_3)_2 \cdot 1/4\text{CH}_3\text{OH}$, in space group $P4_2/n$, with cell dimensions $a = 19.388$ (2) Å, $c = 9.779$ (1) Å, $V_{\text{calcd}} = 3676$ (1) Å³, and $Z = 4$. The structure was solved by the heavy-atom method and was refined by full-matrix least-squares techniques to a final value of $R = 0.0417$ ($R_w = 0.0545$) based upon 1395 observations. The Mn atom is located at a crystallographic inversion center and is six-coordinate with the O-Mn-O unit linear and the MnN_4 unit strictly planar. Bond distances are as follows: two Mn-O bonds, 1.839 (2) Å; two Mn-N1 bonds, 1.993 (3) Å; two Mn-N2 bonds, 2.031 (3) Å; two O-C bonds, 1.387 (3) Å. The magnetic susceptibility of $\text{Mn}^{\text{IV}}\text{TPP}(\text{OCH}_3)_2$ determined in solution and in the solid state at 25 °C gave $\mu_{\text{eff}} = 3.9 \mu_B$. Low-temperature magnetic susceptibility measurements of the solid complex showed Curie-Weiss behavior with $\theta = -0.5$ K and $\mu_{\text{eff}} = 3.91 \pm 0.02 \mu_B$ from 5.0 to 300 K. A high-spin d^3 manganese(IV) porphyrin ground electronic state is assigned to $\text{Mn}^{\text{IV}}\text{TPP}(\text{OCH}_3)_2$ on the basis of structural, magnetic, and infrared spectral properties. The oxidation of $\text{Mn}^{\text{II}}\text{TPP}$ by iodosylbenzene in methanol is also found to yield $\text{Mn}^{\text{IV}}\text{TPP}(\text{OCH}_3)_2$, in contrast to a previous report of the synthesis of $\text{O}=\text{Mn}^{\text{IV}}\text{TPP}$ under similar conditions.

Introduction

High-valent¹ manganese porphyrin complexes are possible intermediates in several systems that utilize manganese porphyrin complexes as catalysts for the oxidation of alkanes, alkenes, alcohols, ethers, and amines to a variety of products.² Oxidized manganese porphyrin complexes have also been shown to evolve hydrogen peroxide or dioxygen in chemical and photochemical reactions.³ The detailed mechanisms of these reactions are unknown. The isolation and determination of the ground electronic states of oxidized manganese porphyrin complexes are critical to the understanding of their reactivity. One dimeric Mn(IV) porphyrin complex has been isolated and crystallographically characterized,⁴ but crystallographic studies of monomeric high-valent manganese porphyrins have not yet appeared.

In this paper we report the isolation and first X-ray crystallographic characterization of a monomeric oxidized manganese porphyrin complex, dimethoxy(5,10,15,20-tetraphenylporphinato)manganese(IV), $\text{Mn}^{\text{IV}}\text{TPP}(\text{OCH}_3)_2$ ⁵ (1). A synthesis of $\text{Mn}^{\text{IV}}\text{TPP}(\text{OCH}_3)_2$ from $\text{Mn}^{\text{II}}\text{TPP}$ in methanol contrasts with an earlier report of the synthesis of the complex $\text{O}=\text{Mn}^{\text{IV}}\text{TPP}$ under similar conditions.⁶ Evaluation of that

report indicates the data used to assign the $\text{O}=\text{Mn}^{\text{IV}}\text{TPP}$ formulation were not conclusive.

Experimental Section

Physical Measurements. Elemental analyses were performed by the microanalytical laboratory, Department of Chemistry, University of California, Berkeley. Infrared spectra were recorded on a Perkin-Elmer 597 spectrophotometer. Electronic spectra were recorded on a Hewlett-Packard 8450A UV-visible spectrometer. Magnetic susceptibility measurements were obtained in solution by the Evans method⁷ using a Varian EM-390 90-MHz NMR spectrometer. Variable-temperature magnetic susceptibility measurements in the solid state were recorded on a SQUID apparatus (SHE Corp. VTS 800 susceptometer), which had been calibrated at room temperature by using a Pt standard. The calibration at low temperatures was verified by reproducing the literature susceptibility values⁸ of $\text{Hg-Co}(\text{SCN})_4$ to within 1% over the temperature range 5–50 K.

Materials. $\text{Mn}^{\text{III}}\text{TPP}(\text{OAc})$ was synthesized by literature methods⁹ and purified by recrystallization, first from acetic acid and then from toluene/heptane. Iodosylbenzene ($\text{C}_6\text{H}_5\text{IO}$, also called iodosobenzene) was synthesized by literature methods.¹⁰ Methanol was distilled from $\text{Mg}(\text{OCH}_3)_2$ under a dry N_2 atmosphere. Dichloromethane, chlorobenzene, and hexane were purified by washing sequentially with H_2SO_4 , water, and dilute aqueous Na_2CO_3 , followed by drying with Na_2SO_4 and distilling from P_2O_5 under N_2 onto activated 4-Å molecular sieves. A 25 wt % solution of NaOCH_3 in methanol (Aldrich, ~4.4 M) and other reagents were used as received.

Methods. Dry and oxygen-free N_2 atmospheres were used routinely, except for the manipulation of solid Mn(III) and Mn(IV) porphyrin complexes. Manipulations under N_2 were performed by using standard Schlenk, cannula, and syringe techniques.

Syntheses of $\text{Mn}^{\text{IV}}\text{TPP}(\text{OCH}_3)_2$. Method 1. Iodosylbenzene Oxidation of $\text{Mn}^{\text{III}}\text{TPP}(\text{OAc})$. $\text{Mn}^{\text{III}}\text{TPP}(\text{OAc})$ (1.8 g, 2.5 mmol) was dissolved in 190 mL of methanol and filtered to give a red solution. Addition of 2.0 mL of ~4.4 M sodium methoxide in methanol gave a green solution. A freshly made and filtered solution of iodosylbenzene (2.0 g, 9 mmol) in methanol (30 mL) was added over a 9-min period to yield a brown solution. The reaction was stirred for 1 h, and the

- (1) "Oxidized" and "high-valent" will be used in this paper to refer to manganese porphyrin complexes more oxidized than the manganese(III) porphyrin oxidation state, the stable oxidation state of manganese porphyrin complexes under aerobic conditions.
- (2) (a) Hill, C. L.; Smegal, J. A. *Now. J. Chim.* **1982**, *6*, 287. (b) Tabushi, I.; Yazaki, A. *J. Am. Chem. Soc.* **1981**, *103*, 7371. (c) Chang, C. K.; Ebina, F. *J. Chem. Soc., Chem. Commun.* **1981**, 778. (d) Perrée-Fauvet, M.; Gaudemer, A. *Ibid.* **1981**, 874. (e) Mansuy, D.; Bartoli, J.-F.; Chottard, J.-C.; Lange, M. *Angew. Chem. Int. Ed. Engl.* **1980**, *19*, 909. (f) Hill, C. L.; Schardt, B. C. *J. Am. Chem. Soc.* **1980**, *102*, 6374. (g) Groves, J. T.; Kruper, W. J., Jr.; Haushalter, R. C. *Ibid.* **1980**, *102*, 6375. (h) Tabushi, I.; Koga, N. *Tetrahedron Lett.* **1979**, 3681. (i) Tabushi, I.; Koga, N. *J. Am. Chem. Soc.* **1979**, *101*, 6456. (j) Tabushi, I.; Koga, N. *Tetrahedron Lett.* **1978**, 5017.
- (3) (a) Carnieri, N.; Harriman, A. *J. Photochem.* **1981**, *15*, 341. (b) Harriman, A.; Porter, G. *J. Chem. Soc., Faraday Trans. 2* **1979**, *75*, 1543. (c) Porter, G. *Proc. R. Soc. London, Ser. A* **1978**, *326*, 281. (d) Tabushi, I.; Kojo, S. *Tetrahedron Lett.* **1975**, 305.
- (4) (a) Schardt, B. C.; Hill, C. L. *J. Chem. Soc., Chem. Commun.* **1981**, 765. (b) Schardt, B. C.; Smegal, J. S.; Hollander, F. J.; Hill, C. L. *J. Am. Chem. Soc.* **1982**, *104*, 3964.
- (5) Abbreviation: TPP^{2-} = dianion of 5,10,15,20-tetraphenylporphyrin.
- (6) Willner, I.; Otvos, J. W.; Calvin, M. *J. Chem. Soc., Chem. Commun.* **1980**, 964.

- (7) Evans, D. F. *J. Chem. Soc.* **1959**, 2003.
- (8) Brown, D. B.; Crawford, V. H.; Hall, J. W.; Hatfield, W. E. *J. Phys. Chem.* **1977**, *81*, 1303.
- (9) Adler, A. D.; Longo, F. R.; Kampas, F.; Kim, J. *J. Inorg. Nucl. Chem.* **1970**, *32*, 2443.
- (10) Lucas, H. J.; Kennedy, E. R.; Formo, M. W. "Organic Syntheses"; Wiley: New York, 1955; Collect. Vol. III, p 483.

resulting precipitate was collected by filtration, rinsed with methanol, and dried in vacuo to yield 1.52 g (2.1 mmol, 84%) of purple flakes. Anal. Calcd for $C_{46}H_{34}N_4MnO_2$: C, 75.71; H, 4.70; N, 7.68. Found: C, 75.45; H, 4.84; N, 7.65.

Method 2. Sodium Hypochlorite Oxidation of $Mn^{III}TPP(OAc)$. $Mn^{III}TPP(OAc)$ (100 mg, 0.14 mmol) was dissolved in 40 mL of methanol. The red solution turned green on addition of 0.30 mL of 4.4 M sodium methoxide in methanol. This solution was filtered and then was treated while being vigorously stirred with 0.35 mL (0.24 mmol) of aqueous 0.7 M sodium hypochlorite. The green solution rapidly turned brown, and precipitation of the product began within 5 min. The mixture was allowed to stand for 1 h. The product was collected by filtration, rinsed with 2 mL of methanol and twice with 1 mL of diethyl ether, and then dried 12 h in vacuo to yield 74 mg (0.10 mmol, 74%) of very fine purple flakes. Anal. Calcd for $C_{46}H_{34}N_4MnO_2$: C, 75.71; H, 4.70; N, 7.68. Found: C, 75.73; H, 4.77; N, 7.85.

Method 3. Iodosylbenzene Oxidation of $Mn^{II}TPP$. $Mn^{III}TPP(OAc)$ (100 mg, 0.14 mmol) was dissolved in 10 mL of methanol under N_2 to give a red solution. When this solution was treated with sodium borohydride (40 mg, 1 mmol), it instantly turned green, and precipitation of purple $Mn^{II}TPP$ flakes began within seconds. After 15 min of stirring, most of the chromophore had precipitated, and the visible spectrum showed reduction was complete ($\lambda_{max} = 432$ nm corresponding to $Mn^{II}TPP$). Iodosylbenzene (100 mg, 0.45 mmol) was added to this mixture. Within 10 s the color of the suspension turned brown, and within 1 min the purple $Mn^{II}TPP$ precipitate appeared to dissolve completely. After the reaction mixture was stirred for 1 h, much precipitate was present, and the visible spectrum showed that oxidation was complete ($\lambda_{max} = 420$ nm corresponding to $Mn^{IV}TPP(OCH_3)_2$). The precipitate was collected, rinsed with three 2-mL portions of methanol and three 2-mL portions of hexane, and dried in vacuo 9 h to give 73 mg (0.10 mmol, 73%) of product.

Synthesis of $Mn^{III}TPP(OCD_3)_2$. A solution of $Mn^{III}TPP(OAc)$ (59 mg, 0.08 mmol) in 4.2 mL of CD_3OD (99.5 atom % D) was treated with 0.25 mL of ~ 2.5 M $LiOCD_3$ in CD_3OD (the $LiOCD_3$ solution was made by cautious addition of a hexane solution of *n*-BuLi into CD_3OD). To this solution was immediately added a filtered solution of iodosylbenzene (65 mg, 0.3 mmol) in CD_3OD (0.9 mL). The reaction was stirred for 2 h. The precipitate was collected, rinsed with 1 mL of CD_3OD , and dried in vacuo to give 50 mg (0.068 mmol, 84%) of a purple microcrystalline solid.

Synthesis of $Mn^{II}TPP \cdot 2CH_3OH$. $Mn^{III}TPP(OAc)$ (0.41 g, 0.56 mmol) was dissolved in 40 mL of methanol. On addition of sodium borohydride (0.19 g, 5 mmol), rapid H_2 evolution occurred. The solution turned green, and purple flakes of the product began to precipitate within 30 s. After 15 min, H_2 evolution had ceased. The air-sensitive product was isolated by filtration, rinsed with two 5-mL portions of methanol, and dried in vacuo for 12 h to yield 0.28 g (0.38 mmol, 68%) of finely divided purple flakes of $Mn^{II}TPP \cdot 2CH_3OH$. Anal. Calcd for $C_{46}H_{36}N_4O_2Mn$: C, 75.50; H, 4.96; N, 7.66. Found: C, 75.72; H, 4.89; N, 7.71.

Since the calculated analyses for $Mn^{II}TPP \cdot 2CH_3OH$ and $Mn^{II}TPP(OCH_3)_2$ are similar, the IR spectrum of the product was recorded after the analysis to check the possibility of oxidation of the complex in the solid state to $Mn^{IV}TPP(OCH_3)_2$. The absence of characteristic methoxide IR absorbances at 2888, 2855, 2775, and 1050 cm^{-1} eliminated this possibility.

Spectroscopic Experiments. Spectroscopic studies were performed in dilute (0.20 mM) methanol solution to prevent precipitation of the manganese porphyrin complexes. The visible spectrum of 0.20 mM $Mn^{III}TPP(OAc)$ in methanol is given in Figure 1a.

(1) A 100-mL solution of 0.20 mM $Mn^{III}TPP(OAc)$ in methanol was treated with 80 mg (2.1 mmol) of sodium borohydride. Rapid H_2 evolution occurred, and after 10 min, the visible spectrum showed that reduction to $Mn^{II}TPP$ was complete (Figure 1b). The solution was stirred 1 h, and then 250 mg (1.1 mmol) of iodosylbenzene was added. The solution turned brown, and after 30 min, the visible spectrum showed that oxidation was complete (Figure 1c). The treatment of 1 mL of this solution with 5 μ L of acetic acid caused reduction to occur over 30 min to give a 0.19 mM solution of $Mn^{III}TPP(OAc)$ (based upon the visible spectrum). This result indicates that approximately 95% of the chromophore was intact after this sequence of reactions. The bulk solution that was not treated with acetic acid remained 95% oxidized after 24 h.

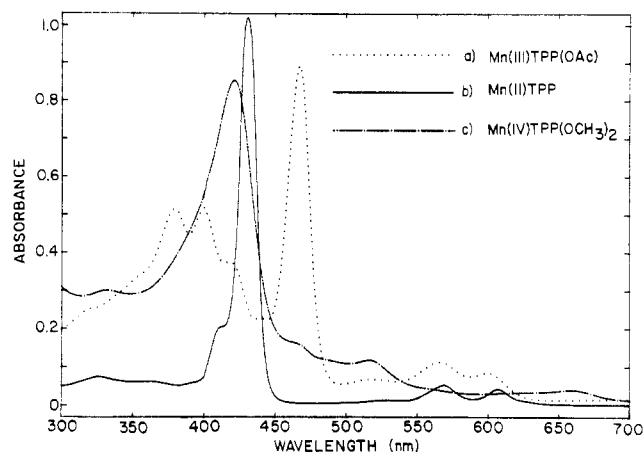


Figure 1. Spectroscopic experiment 1: (a) electronic spectrum of 0.2 mM $Mn^{III}TPP(OAc)$ in methanol; (b) electronic spectrum of $Mn^{II}TPP$ obtained 10 min after treating 100 mL of 0.20 mM $Mn^{III}TPP(OAc)$ with 80 mg of $NaBH_4$ (absorbance in this spectrum only is reduced by a factor of 3); (c) electronic spectrum 30 min after treating this solution with 250 mg of iodosylbenzene. All spectra were obtained in 0.5-mm path length cells.

(2) A vigorously stirred 100-mL solution of 0.20 mM $Mn^{III}TPP(OAc)$ in methanol was treated with 250 mg (1.1 mmol) of iodosylbenzene. After 25 min, the visible spectrum still corresponded to 98% $Mn^{III}TPP(OAc)$, indicating that insignificant amounts of oxidized products were present. The addition of 0.5 mL (2.2 mmol) of 4.4 M $NaOCH_3$ in methanol caused complete oxidation to occur within 20 min to give a spectrum identical with that in Figure 1c.

(3) A 100-mL solution of 0.20 mM $Mn^{III}TPP(OAc)$ was treated with 80 mg (2.1 mmol) of sodium borohydride to give $Mn^{II}TPP$. When this solution was left in a serum-stoppered volumetric flask under N_2 for 24 h, reoxidation of the $Mn^{II}TPP$ to a $Mn^{III}TPP$ complex occurred¹¹ and a visible spectrum identical with that of 0.20 mM $Mn^{III}TPP(OAc)$ was observed. When this solution was treated with 250 mg (1.1 mmol) of iodosylbenzene, complete oxidation occurred in 20 min to give a visible spectrum identical with that in Figure 1c.

X-ray Crystallography. Crystal Growth. Crystals were grown by the diffusion of a heptane layer into a 1:1 dichloromethane/methanol solution of $Mn^{III}TPP(OCH_3)_2$ at -30 °C.

Collection and Reduction of Intensity Data. A fragment of a needle-like crystal $\sim 0.12 \times 0.13 \times 0.42$ mm was mounted on a glass fiber, in air, by using polycyanoacrylate glue. Preliminary precession photographs indicated tetragonal Laue symmetry $4/m$. Data were collected on an Enraf-Nonius CAD-4 diffractometer. Automatic search and indexing yielded a primitive tetragonal cell.¹² Intensity data confirmed the Laue symmetry, and systematic absences ($00l$, $l \neq 2n$; $hk0$, $h + k \neq 2n$) were consistent only with space group $P4_2/n$ (No. 86). Determination of accurate cell dimensions and orientation proceeded normally. Crystal parameters and data collection procedures are given in Table I.

Structure Solution and Refinement. The 2794 intensity data were converted to structure factor magnitudes and their esd's by correction for background, scan speed, and Lorentz and polarization factors.¹³⁻¹⁵

- (11) The mechanism by which the $Mn^{II}TPP$ is reoxidized to $Mn^{III}TPP$ in methanol is not understood at this time. Since $Mn^{II}TPP$ is very oxygen sensitive, the diffusion of 5 μ mol of O_2 through the serum stopper would be sufficient to completely oxidize all $Mn^{II}TPP$ back to $Mn^{III}TPP$ species.
- (12) Instrumentation at the University of California Chemistry Department X-ray Crystallographic Facility consists of two Enraf-Nonius CAD-4 diffractometers, one controlled by a DEC PDP 8/a with a RK05 disk and the other by a DEC PDP 8/e with an RL01 disk. Both use Enraf-Nonius software as described in: "CAD-4 Operation Manual"; Enraf-Nonius: Delft, Nov 1977, updated Jan 1980.
- (13) All calculations were performed on a PDP 11/60 using locally modified Nonius-SDP¹⁴ software.
- (14) "Structure Determination Package User's Guide"; Molecular Structure Corp: College Station, TX 77840, April 1980.

Table I. Crystal and Data Collection Parameters for MnTPP(OCH₃)₂·1/4CH₃OH

(A) Crystal Parameters at 25 °C ^{a,b}	
formula	C _{46.25} H _{34.75} N ₄ O _{2.25} Mn
fw	737.8
space group	P4 ₂ /n (No. 86)
a, Å	19.388 (2)
c, Å	9.7794 (12)
V, Å ³	3676 (1)
Z	4
d(calcd), g cm ⁻³	1.333
cryst dimens, mm	0.12 × 0.13 × 0.42
μ(calcd), cm ⁻¹	4.2
(B) Data Collection	
diffractometer	Enraf-Nonius CAD-4
radiation	Mo Kα (λ = 0.71073 Å)
monochromator	highly oriented graphite (2θ _m = 12.2°); perpendicular mode, assumed 50% perfect
reflcs measd	+h, +k, +l
scan type	θ-2θ
2θ range	3-45°
scan speed, deg min ⁻¹	0.43-5.0
scan width, deg	Δθ = 0.50 + 0.347 tan θ
bkgd	added 25% of scan width at end of each scan
reflcs collected	2794
unique reflcs	2397
intens standards	(12,4,0), (4,12,0), and (006); measured every 2 h of X-ray exposure time; over the period of data collection no observed decay in intensity
orientation	3 reflections checked after every 500 measurements; crystal orientation redetermined if any of the reflections were offset from their predicted positions by more than 0.1°; reorientation not performed during data collection

^a Unit cell parameters and their esd's were derived by a least-squares fit to the setting angles of the unresolved Mo Kα components of 24 reflections with 2θ near 26°. ^b In this and all subsequent tables the esd's of all parameters are given in parentheses, right-justified to the least significant digit(s) given.

Analysis of the intensities of several reflections located near χ = 90°, which were collected at 10° increments of rotation about the diffraction vector, gave a ratio of 1.026 for maximum/minimum intensity. No absorption correction was performed. Systematic absences were removed from the data set, and symmetry-equivalent data were averaged (4/m symmetry) to yield 2397 unique reflections, of which 1411 had values of F² greater than 3 times their esd's. With only four molecules per unit cell, the molecule must possess crystallographic point symmetry. Analysis of the intensities indicated a strong pseudoabsence condition on hkl, h + k = 2n, k + l = 2n, and h + l = 2n, consistent only with placement of the molecule on the special positions 4c or 4d (point symmetry $\bar{1}$). A three-dimensional Patterson map indicated that the TPP core was approximately in the ab plane and a ligating atom was near the manganese both above and below

(15) The data reduction formulas are

$$F_o^2 = \frac{\omega}{Lp}(C - 2B) \quad \sigma_o(F_o^2) = \frac{\omega}{Lp}(C + 4B)^{1/2}$$

$$F_o = (F_o^2)^{1/2} \quad \sigma_o(F) = \sigma_o(F_o^2)/2F_o$$

where C is the total count in the scan, B is the sum of the two background counts, ω is the scan speed used in deg/min, and

$$\frac{1}{Lp} = \frac{(\sin 2\theta)(1 + \cos^2 2\theta_m)}{1 + \cos^2 2\theta_m - \sin^2 2\theta}$$

is the correction for Lorentz and polarization effects for a reflection with scattering angle 2θ and radiation monochromatized with a 50% perfect single-crystal monochromator with scattering angle 2θ_m.

Table II. Final Positional Parameters for the Non-Hydrogen Atoms of MnTPP(OCH₃)₂·1/4CH₃OH

atom	x	y	z
MN	0.0000 (0)	0.0000 (0)	0.0000 (0)
O1	0.0147 (1)	-0.0056 (1)	0.1854 (3)
OH	0.2190 (0)	0.2360 (0)	0.3320 (0)
N1	0.0895 (2)	0.0499 (2)	-0.0145 (3)
N2	-0.0517 (2)	0.0906 (2)	0.0186 (3)
C1	0.1553 (2)	0.0233 (2)	-0.0211 (4)
C2	0.2058 (2)	0.0754 (2)	-0.0190 (5)
C3	0.1720 (2)	0.1362 (2)	-0.0092 (4)
C4	0.1000 (3)	0.1215 (2)	-0.0061 (4)
C5	0.0481 (2)	0.1702 (2)	0.0098 (4)
C6	-0.0204 (2)	0.1544 (2)	0.0218 (4)
C7	-0.0770 (2)	0.2046 (2)	0.0309 (5)
C8	-0.1356 (2)	0.1714 (2)	0.0372 (5)
C9	-0.1206 (2)	0.0989 (2)	0.0274 (4)
C10	0.1706 (2)	-0.0475 (2)	-0.0287 (4)
C11	0.0680 (2)	0.2448 (2)	0.0166 (4)
C12	0.0599 (2)	0.2824 (2)	0.1361 (5)
C13	0.0773 (2)	0.3518 (2)	0.1404 (5)
C14	0.1052 (3)	0.3841 (3)	0.0275 (5)
C15	0.1129 (2)	0.3468 (2)	-0.0906 (5)
C16	0.0957 (3)	0.2778 (2)	-0.0974 (5)
C17	0.2444 (2)	-0.0689 (2)	-0.0352 (4)
C18	0.2828 (2)	-0.0567 (2)	-0.1505 (5)
C19	0.3529 (2)	-0.0756 (3)	-0.1546 (5)
C20	0.3820 (2)	-0.1044 (2)	-0.0435 (6)
C21	0.3438 (3)	-0.1183 (3)	0.0711 (6)
C22	0.2755 (2)	-0.0982 (2)	0.0751 (5)
C23	-0.0291 (3)	0.0166 (3)	0.2887 (5)
CH3	0.2620 (0)	0.2550 (0)	0.2190 (0)

the plane. The manganese was placed at the origin of the cell (position 4c), and the atoms of the central (C₂₀N₄) core of the TPP were oriented around it, on the basis of the positions of the Mn-N vectors in the Patterson map. Refinement and location of additional non-hydrogen atoms proceeded normally via least-squares and Fourier techniques. After the axial methoxide ligands were refined, it became evident that normal procedures were not working well. Attempted refinements of all non-hydrogen atoms with anisotropic thermal parameters repeatedly yielded non-positive-definite thermal tensors. The problem was solved by shifting from the normal weighting scheme¹⁶ to unit weights. Using unit weights for all reflections with F_o² > 3σ(F_o²), we obtained residuals¹⁶ of R = 7.52% and R_w = 7.79% at convergence with all non-hydrogen atoms anisotropic. A difference Fourier map phased by these atoms revealed two relatively large (0.8 e/Å³) peaks near the site of the $\bar{4}$ point symmetry at 1/4, 1/4, 1/4 and peaks located near all positions where TPP hydrogens would be expected. Idealized hydrogen positions were calculated (C-H = 0.95 Å), and the contribution of the hydrogen atoms to the structure factor calculations was included, although they were not allowed to refine. Refinement with unit weights converged with R = 5.48%, R_w = 6.08%, and R_{all} = 11.45%.

A return to the usual weighting scheme¹⁶ and analysis of the residuals in groups showed that (1) the 002 reflection suffered extremely from secondary extinction, but no other reflections were so affected, (2) the weighted residuals of those reflections with 2θ < 10° were uniformly very large, and (3) the values of the residuals were very dependent on the parity grouping (see below).

(16) Residuals and goodness of fit are defined as

$$R = \frac{\sum ||F_o| - |F_c||}{\sum |F_o|} \quad R_w = \left(\frac{\sum w(|F_o| - |F_c|)^2}{\sum w F_o^2} \right)^{1/2}$$

$$\text{GOF} = \left(\frac{\sum w(|F_o| - |F_c|)^2}{n_o - n_v} \right)^{1/2}$$

where n_o is the number of observations, n_v is the number of variable parameters, and the weights w were given by

$$w = \frac{4F_o^2}{\sigma^2(F_o^2)} \quad \sigma^2(F_o^2) = \sigma_o^2(F_o^2) + (pF)^2$$

where p is the factor used to lower the weight of intense reflections.

On the basis of (1) and (2), it was decided to eliminate the 20 reflections with $(\sin \theta)/\lambda < 0.11$ (which included the (002)) and to refine by using the normal weighting scheme. This refinement converged with $R = 5.08\%$, $R_w = 7.12\%$, and $GOF = 3.77$ for 241 parameters refined against 1395 observations.

The two largest peaks in the difference Fourier were then interpretable as a partial-occupancy methanol molecule, disordered around the $\bar{4}$ point symmetry operation at $1/4, 1/4, 1/4$. Idealized positions for the carbon and oxygen were calculated on the basis of a C–O bond distance of 1.43 Å. These were included in the least-squares refinements with fixed positions and fixed isotropic thermal parameters equal to 8.0 \AA^2 . Their joint occupancy was allowed to vary. Convergence was reached with a refined value of the occupancy of 0.121 (3), corresponding to approximately 1 molecule of methanol per unit cell or $1/4$ molecule of CH_3OH per molecule of complex (the presence of the methanol solvate was independently verified by GC analysis of the crystalline complex dissolved in dichloromethane and injected into a 4-ft Poropak QS column operated at 85°C).

The final residuals for 242 variables refined against the 1395 data for which $F^2 > 3\sigma(F^2)$ and $(\sin \theta)/\lambda > 0.11$ were $R = 4.17\%$, $R_w = 5.45\%$, and $GOF = 2.89$. The R value for all 2397 data was 10.4%.

The largest peak in the final difference Fourier map had an electron density of 0.31 e/\AA^3 located between the Mn atom and N1. There was no residual density near the methanol or the other $\bar{4}$ position in the unit cell.

The quantity minimized by the least-squares program was $\sum w(|F_o| - |F_c|)^2$, where w is the weight of the given observation. The p factor,¹⁶ used to reduce the intensity of the reflections, was set to 0.02 in the final cycles of refinement. The analytical forms for the scattering factor tables for the neutral atoms were used,¹⁷ and all non-hydrogen scattering factors were corrected for both the real and imaginary components of anomalous dispersion.¹⁸

The final positional parameters of the non-hydrogen atoms are given in Table II. The thermal parameters of the non-hydrogen atoms, the positions of the hydrogen atoms, and a listing of the values of F_o and F_c are available as supplementary material.

The refinement of the structure and the final analysis of the residuals were made more difficult by the strong pseudoabsence condition present in the structure. Those reflections allowed by the face-centering pseudooperation had average values of F of 43.7 for the parity eee and 39.9 for the parity ooo . Those reflections not allowed by the centering pseudooperation fell into two classes, both weak. Those groups with h and k of different parity (oeo , oee , ooo , and oee) had an average F between 9.9 and 13.6, but two groups (ooe and ooo) had an average F of 4.9 and 3.5, about one-tenth the average for the allowed reflections. These latter two groups also have the worst residuals of any of the parity groups, $R = 12.9\%$ and 14.4% , respectively, while the group residuals for the "allowed" eee and ooo parities are 3.04% and 3.15%, respectively.

This strong variation in agreement across parity groups is representative of some of the problems of solving structures involving high pseudosymmetry. However, the generally low value of the residuals for most of the reflections and the normal trends with respect to the grouping of reflections in the ranges of $(\sin \theta)/\lambda$ and $|F_o|$ indicate our model does not misrepresent the data in any gross manner.

The poor agreement of the low $(\sin \theta)/\lambda$ data persisted even to the end of the refinement ($\text{rms}(\Delta F/\sigma(F)) = 31.4\%$). We have no explanation for this, especially as the worst agreements were not apparently dependent on F_o or parity for these low-angle reflections. A list of the 20 low-angle data rejected from the least-squares procedures is given at the end of Table SVI.¹⁹

Results

Syntheses and Stability of $\text{Mn}^{\text{IV}}\text{TPP}(\text{OCH}_3)_2$. The oxidation of $\text{Mn}^{\text{III}}\text{TPP}(\text{OAc})$ in basic methanol, using either iodobenzene or sodium hypochlorite as the oxidant, yields analytically pure $\text{Mn}^{\text{IV}}\text{TPP}(\text{OCH}_3)_2$. In the solid state, $\text{Mn}^{\text{IV}}\text{TPP}(\text{OCH}_3)_2$ appears to be indefinitely stable at 25°C .

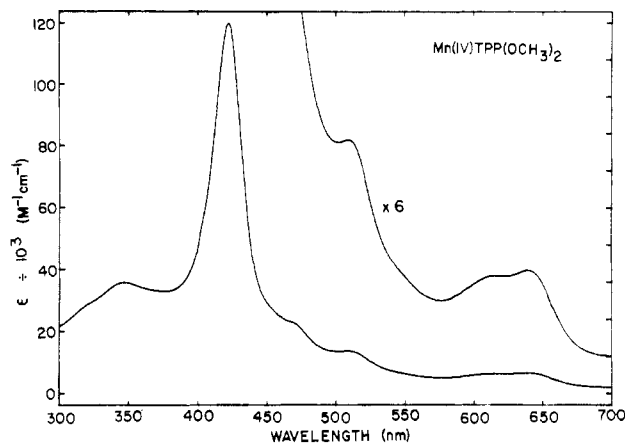


Figure 2. Quantitative electronic spectrum of 0.20 mM $\text{Mn}^{\text{IV}}\text{TPP}(\text{OCH}_3)_2$ in dichloromethane (0.5-mm path length cell).

Isolated $\text{Mn}^{\text{IV}}\text{TPP}(\text{OCH}_3)_2$ could not be completely redissolved in methanol without significant decomposition. In purified, dry dichloromethane, isolated $\text{Mn}^{\text{IV}}\text{TPP}(\text{OCH}_3)_2$ can be rapidly and completely dissolved (<15 s; see visible spectrum, Figure 2), but reduction to a Mn^{III} porphyrin ($\lambda_{\text{max}} = 468$ nm) occurs over a 2-h period. If the dichloromethane is not rigorously free of HCl, reduction to $\text{Mn}^{\text{III}}(\text{TPP})\text{Cl}$ ($\lambda_{\text{max}} = 478$ nm) occurs in minutes.

IR Spectra of $\text{MnTPP}(\text{OCH}_3)_2$.¹⁹ Samples of $\text{MnTPP}(\text{OCH}_3)_2$ made by methods 1, 2, and 3 all gave the same infrared spectrum (KBr pellet, ~ 5 wt %). No new bands are observed in the region 1250 – 1300 cm^{-1} , where diagnostic tetraphenylporphyrin π -cation-radical absorptions are believed to occur.²⁰ In addition to exhibiting absorptions normally found in manganese tetraphenylporphyrin complexes, the IR spectrum of $\text{MnTPP}(\text{OCH}_3)_2$ exhibited characteristic methoxide absorptions. The assignments of these bands were verified by synthesis and determination of the IR spectrum¹⁹ of the deuterated complex $\text{MnTPP}(\text{OCD}_3)_2$. The methoxide C–H stretches at 2888 , 2855 , and 2775 cm^{-1} completely disappeared upon deuteration and were replaced by C–D stretches at 2198 , 2167 , and 2026 cm^{-1} . The methoxy C–O stretch²¹ at 1050 cm^{-1} shifted upon deuteration to become a shoulder at 1020 cm^{-1} (superimposed on a strong porphyrin band at 1005 cm^{-1}) as expected (shifts of 30 – 40 cm^{-1} are usually observed upon deuteration of methoxide complexes²¹). The Mn–O stretch at 550 cm^{-1} in **1** shifted to 532 cm^{-1} in $\text{MnTPP}(\text{OCD}_3)_2$ (this shift is also reasonable for the deuteration of a metal-bound methoxy group²¹). What is believed to be a C–H bend at 1420 cm^{-1} disappeared and was replaced by a band at 1090 cm^{-1} . An attempt was made to record the IR spectrum of a saturated solution of $\text{MnTPP}(\text{OCH}_3)_2$ in CCl_4 (0.2-mm path length). However, peak intensities were insufficient for peak assignments due to the low solubility of $\text{MnTPP}(\text{OCH}_3)_2$ in this solvent.

Magnetic Susceptibility. The magnetic susceptibility of $\text{Mn}^{\text{IV}}\text{TPP}(\text{OCH}_3)_2$ determined in solution (3.08 mM in 22:2:1 chlorobenzene/acetonitrile/ Me_4Si by volume) at room temperature gave $\mu_{\text{eff}} = 3.9 \pm 0.1 \mu_{\text{B}}$ on the basis of the equation $\mu_{\text{eff}} = 2.83(\chi_{\text{M}}T)^{1/2}$ and the diamagnetic correction for the porphyrin ring²² of $-700 \times 10^{-6} \text{ cgsu mol}^{-1}$. The variable-temperature magnetic susceptibility was determined in the solid state at a field strength of 20 000 G. After the application of the above diamagnetic correction, a plot of $1/\chi_{\text{M}}$ vs. tem-

(17) Cromer, D. T.; Waber, J. T. "International Tables for X-ray Crystallography"; Kynoch Press: Birmingham, England, 1974; Vol. IV, Table 2.2B.

(18) Cromer, D. T. "International Tables for X-ray Crystallography"; Kynoch Press: Birmingham, England, 1974; Vol. IV, Table 2.3.1.

(19) Available as supplementary material.

(20) Shimomura, E. T.; Philippi, M. A.; Goff, H. M.; Scholz, W. F.; Reed, C. A. *J. Am. Chem. Soc.* **1981**, *103*, 6778.

(21) Maslowsky, E. "Vibrational Spectra of Organometallic Compounds"; Wiley: New York, 1977.

(22) Eaton, S. S.; Eaton, G. R. *Inorg. Chem.* **1980**, *19*, 1095.

perature yielded a straight line with a temperature intercept of -0.5 K, indicating Curie-Weiss behavior. With use of the experimental Weiss constant of -0.5 K and the equation $\mu_{\text{eff}} = 2.83(\chi_M(T - \Theta))^{1/2}$, values within the range $\mu_{\text{eff}} = 3.91 \pm 0.02 \mu_B$ were calculated¹⁹ for all data points from 5.0 to 300 K.

Mass Spectrum. The mass spectrum of $\text{Mn}^{\text{IV}}\text{TPP}(\text{OCH}_3)_2$ was determined by field-desorption mass spectrometry, base peak m/e 667 (100%) corresponding to $[\text{MnTPP}]^+$. No peaks $>2\%$ of this peak height were observed above m/e 670.

Attempted Synthesis of $\text{O}=\text{Mn}^{\text{IV}}\text{TPP}$. The reaction of $\text{Mn}^{\text{III}}\text{TPP}(\text{OAc})$ with iodosylbenzene in methanol has been reported to give no change in the visible spectrum. It was reported that, after the reduction of $\text{Mn}^{\text{III}}\text{TPP}(\text{OAc})$ by sodium borohydride to give $\text{Mn}^{\text{II}}\text{TPP}$, the addition of iodosylbenzene to the reaction mixture caused oxidation to occur to give a product formulated as $\text{O}=\text{Mn}^{\text{IV}}\text{TPP}$.⁶ The experimental details of these reactions have not been published.

We have reinvestigated these reactions and find changes in the visible spectra similar to those previously reported (see Figure 1). The reduction of $\text{Mn}^{\text{III}}\text{TPP}(\text{OAc})$ using sodium borohydride gives $\text{Mn}^{\text{II}}\text{TPP}$ (Figure 1b), and in a preparative reaction we have isolated analytically pure $\text{Mn}^{\text{II}}\text{TPP} \cdot 2\text{CH}_3\text{OH}$. When $\text{Mn}^{\text{II}}\text{TPP}$ was formed in situ by sodium borohydride reduction of $\text{Mn}^{\text{III}}\text{TPP}(\text{OAc})$ and subsequently reacted with iodosylbenzene, a visible spectrum indicative of oxidation and similar to that previously assigned to $\text{O}=\text{Mn}^{\text{IV}}\text{TPP}$ was observed (Figure 1c). When this reaction was repeated on a preparative scale, an oxidized Mn porphyrin product was obtained. The IR spectrum (KBr pellet) of the product that we isolated showed it to be $\text{Mn}^{\text{IV}}\text{TPP}(\text{OCH}_3)_2$. This result differs from the previously reported synthesis of the complex $\text{O}=\text{Mn}^{\text{IV}}\text{TPP}$ under similar conditions.⁶ The formulation of an $\text{O}=\text{Mn}^{\text{IV}}\text{TPP}$ species was based upon infrared and mass spectral data.⁶ The CCl_4 solution IR spectrum of the product assigned as $\text{O}=\text{Mn}^{\text{IV}}\text{TPP}$ was reported to show an absorption at 1060 cm^{-1} , which was assigned to a $\text{Mn}=\text{O}$ stretch. The decrease in the intensity of this band at 1060 cm^{-1} and the increase in the intensity of a band at 1000 cm^{-1} upon 30% ^{18}O labeling of the complex were consistent with this formulation. Since strong porphyrin absorptions at 1070 and 1000 cm^{-1} and a strong alkoxide C-O stretch at 1050 cm^{-1} occur in the infrared spectrum of $\text{Mn}^{\text{IV}}\text{TPP}(\text{OCH}_3)_2$, a comparison of the spectra of $\text{O}=\text{Mn}^{\text{IV}}\text{TPP}$ and $\text{Mn}^{\text{IV}}\text{TPP}(\text{OCH}_3)_2$ was needed.

The authors of the previously reported synthesis of $\text{O}=\text{Mn}^{\text{IV}}\text{TPP}$ have kindly provided the unpublished CCl_4 solution IR spectrum of the 30% ^{18}O -labeled $\text{O}=\text{Mn}^{\text{IV}}\text{TPP}$ used in their study.⁶ Several prominent IR absorptions characteristic of TPP complexes were absent from this spectrum (e.g., no characteristic TPP bands were observed near 1370 cm^{-1} ²³), indicating insufficient amounts of porphyrin complexes were present for IR studies. The absence of porphyrin bands may have been due to the low solubility of the manganese porphyrin product in this solvent (e.g., a saturated solution of $\text{Mn}^{\text{IV}}\text{TPP}(\text{OCH}_3)_2$ in CCl_4 gives extremely weak IR bands). The presence of iodobenzene bands was reported in the CCl_4 solution IR spectrum of $\text{O}=\text{Mn}^{\text{IV}}\text{TPP}$. We have compared the IR spectrum of iodobenzene¹⁹ in CCl_4 with the IR spectrum of the 30% ^{18}O -labeled product. Iodobenzene in CCl_4 (1% v/v) exhibits strong absorptions at 1061 , 1017 , and 999 cm^{-1} . The similarity of the ratios of the 1061 -, 1017 -, and 999-cm^{-1} bands in the spectrum of the iodobenzene standard and those of the labeled product indicates that the bands reported at 1060 , 1023 , and 1000 cm^{-1} were probably also due to iodobenzene.

The largest peak reported in the mass spectrum of $\text{O}=\text{Mn}^{\text{IV}}\text{TPP}$ ⁶ occurred at m/e 667 and corresponds to

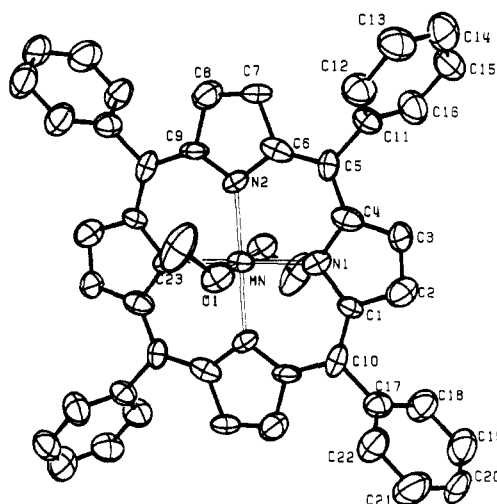


Figure 3. ORTEP²⁶ drawing of the $\text{MnTPP}(\text{OCH}_3)_2$ molecule. Vibrational ellipsoids represent 50% probability surfaces. Hydrogen atoms are omitted for clarity.

$[\text{MnTPP}]^+$, consistent with the known gas-phase reduction of many metalloporphyrins to the divalent state.²⁴ The mass spectrum of $\text{Mn}^{\text{IV}}\text{TPP}(\text{OCH}_3)_2$ gives only the m/e 667 $[\text{MnTPP}]^+$ parent ion. A very weak m/e 683 peak reported for $\text{O}=\text{Mn}^{\text{IV}}\text{TPP}$ is consistent with a $[\text{O}=\text{MnTPP}]^+$ ion but can also be due to partial hydroxylation of the porphyrin periphery by excess oxidant. Reduction of this hydroxylated complex in the gas phase to the divalent complex $\text{Mn}^{\text{II}}(\text{TPP}-\text{OH})$ would give the same m/e as was reported for $\text{O}=\text{Mn}^{\text{IV}}\text{TPP}$.

The oxidation of $\text{Mn}^{\text{II}}\text{TPP}$ by iodosylbenzene was suggested to occur via an oxygen atom transfer from iodosylbenzene to the Mn(II) center to give $\text{O}=\text{Mn}^{\text{IV}}\text{TPP}$.⁶ We will show in a separate paper that iodosylbenzene solvolyzes in methanol to form the complex dimethoxyphenyliodine(III), $\text{C}_6\text{H}_5\text{I}(\text{O}-\text{CH}_3)_2$.²⁵ This reaction may prevent oxygen atom transfer in methanolic solutions. The apparent requirement for the manganese porphyrin complex to be reduced to the divalent state before oxidation by iodosylbenzene occurred was actually due to the need for the solution to be basic before oxidation becomes favorable. As was previously reported,⁶ we find that $\text{Mn}^{\text{III}}\text{TPP}(\text{OAc})$ is not significantly oxidized in the presence of iodosylbenzene in neutral methanol. However, the oxidation of $\text{Mn}^{\text{III}}\text{TPP}(\text{OAc})$ by iodosylbenzene occurs rapidly when the solution is made basic. This result demonstrates that the reduction to a Mn(II) porphyrin complex is not necessary for oxidation by iodosylbenzene and that basic conditions are required for the oxidation of $\text{Mn}^{\text{III}}\text{TPP}$ by iodosylbenzene in methanol. Since $\text{Mn}^{\text{IV}}\text{TPP}(\text{OCH}_3)_2$ is isolated in an analytically pure form and in high yield when this reaction is run under preparative conditions and the visible spectra observed in solution under both preparative and spectroscopic (i.e., dilute) conditions are the same, we conclude that the visible spectrum in Figure 1c corresponds to $\text{Mn}^{\text{IV}}\text{TPP}(\text{OCH}_3)_2$.

If $\text{Mn}^{\text{III}}\text{TPP}(\text{OAc})$ is reduced by sodium borohydride in neutral methanol, the solution becomes more basic due to the reaction of NaBH_4 with the solvent. If the $\text{Mn}^{\text{II}}\text{TPP}$ that is formed is allowed to oxidize back to $\text{Mn}^{\text{III}}\text{TPP}$ in solution¹¹ and the solution is then treated with iodosylbenzene, oxidation occurs to give a visible spectrum corresponding to $\text{Mn}^{\text{IV}}\text{TPP}(\text{OCH}_3)_2$ (identical with Figure 1c). This demonstrates that

(24) (a) Edwards, L.; Dolphin, D. H.; Gouterman, M.; Adler, A. D. *J. Mol. Spectrosc.* **1971**, *38*, 16. (b) Boucher, L. J. *Coord. Chem. Rev.* **1972**, *311*.

(25) Schardt, B. C.; Hill, C. L., manuscript in preparation. The complex $\text{C}_6\text{H}_5\text{I}(\text{OCH}_3)_2$ has been characterized by ^1H NMR, elemental analysis, and infrared spectroscopy.

(23) Alben, J. O.; Choi, S. S.; Adler, A. D.; Caughey, W. S. *Ann. N.Y. Acad. Sci.* **1973**, *206*, 278.

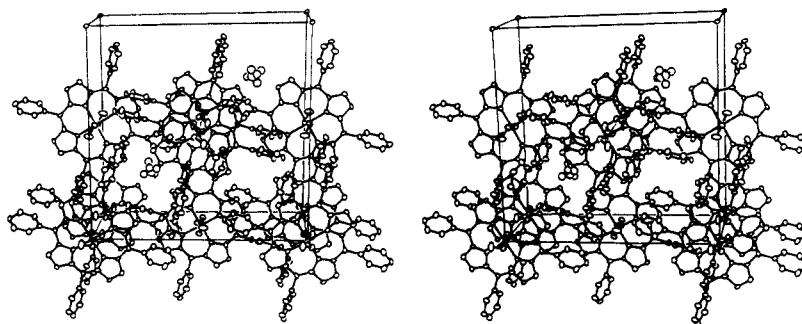


Figure 4. Stereoview of the crystal-packing diagram of $\text{MnTPP}(\text{OCH}_3)_2 \cdot \frac{1}{4}\text{CH}_3\text{OH}$ (20% probability ellipsoids are shown).

the reaction of sodium borohydride with methanol makes the solution sufficiently basic to make the oxidation of $\text{Mn}^{\text{III}}\text{TPP}$ by iodosylbenzene favorable. The addition of acetic acid to $\text{Mn}^{\text{IV}}\text{TPP}(\text{OCH}_3)_2$ in methanol induces reduction back to $\text{Mn}^{\text{III}}\text{TPP}(\text{OAc})$, indicating that $\text{Mn}^{\text{IV}}\text{TPP}(\text{OCH}_3)_2$ in methanol is unstable toward reduction under acidic conditions.

Since the visible spectrum of $\text{Mn}^{\text{IV}}\text{TPP}(\text{OCH}_3)_2$ is obtained when either $\text{Mn}^{\text{II}}\text{TPP}$ or $\text{Mn}^{\text{III}}\text{TPP}$ complexes are oxidized in methanol under basic conditions and $\text{Mn}^{\text{IV}}\text{TPP}(\text{OCH}_3)_2$ is the isolated product from these reactions when they are run under preparative conditions, we conclude that the major species formed in these reactions is $\text{Mn}^{\text{IV}}\text{TPP}(\text{OCH}_3)_2$.

Description of Structure. The ORTEP²⁶ drawing of the $\text{MnTPP}(\text{OCH}_3)_2$ molecule showing the atom-numbering scheme is given in Figure 3, and the stereoview of the crystal-packing diagram is illustrated in Figure 4. Selected interatomic distances and angles are given in Table III.

The crystal structure consists of well-separated molecules of **1** that pack to leave channels in the crystal lattice (Figure 4). The positions of the manganese atoms define a face-centered lattice. The deviations of the rest of the TPP core from an idealized face-centered structure (i.e., with the TPP core normal to *c*) are less than 0.30 Å (except for C8, which deviates by 0.36 Å). The major deviations of the structure from the face-centering symmetry are the tilt of the phenyl rings with respect to the TPP core and the presence of the methanol solvate.

The fourfold disordered $\frac{1}{4}\text{CH}_3\text{OH}$ solvate partially occupies the channels in the crystal lattice at the $\bar{4}$ position. The shortest intermolecular contacts to the hydroxyl end of the methanol solvate are 2.96 (to C3), 3.38 (to C13), and 3.43 Å (to C12). The shortest contacts to the methyl end are 3.33 (to C3) and 3.62 Å (to C12). The methanol is probably not further disordered by the interchange of the methyl and hydroxyl moieties. All intermolecular contacts less than 3.75 Å are given in Table 19.

The $\text{MnTPP}(\text{OCH}_3)_2$ unit has a crystallographically imposed center of symmetry. Thus, the O–Mn–O unit defined by the two ligating methoxide ligands is linear, and the Mn–N₄ unit defined by the four ligating porphyrin nitrogen atoms is strictly planar. The Mn–N₄ unit is tilted 6.5° with respect to the crystallographic *ab* plane, and the O–Mn–O vector lies at an angle of 9.5° with respect to the crystallographic *c* axis and an angle of 3.0° with respect to the normal of the Mn–N₄ plane. Deviations of the atoms in the porphyrin core from the Mn–N₄ plane are less than 0.2 Å. The pyrrole rings are planar to within 3σ (0.012 Å) and are tilted 4.3° (pyrrole containing N1) and 2.6° (pyrrole containing N2) from the Mn–N₄ plane. The methoxy group is rotated 34.0° from the O1–Mn–N2 plane. The planes of the phenyl groups are rotated from the Mn–N₄ plane by 66.6° (phenyl group containing C11) and 70.3° (phenyl group containing C17).

Table III. Bond Distances (Å) and Bond Angles (Deg) in $\text{MnTPP}(\text{OCH}_3)_2$ ^{a-c}

Mn–N1	1.993 (3)	C10–C1	1.406 (4)
Mn–N2	2.031 (3)	C10–C9'	1.391 (5)
Mn–O1	1.839 (2)	C10–C17	1.490 (4)
N1–C1	1.377 (4)	O1–C23	1.387 (3)
N1–C4	1.405 (5)	C11–C12	1.386 (4)
N2–C6	1.379 (4)	C12–C13	1.386 (4)
N2–C9	1.348 (4)	C13–C14	1.380 (5)
C1–C2	1.408 (5)	C14–C15	1.370 (5)
C3–C4	1.424 (6)	C15–C16	1.381 (4)
C6–C7	1.471 (5)	C16–C11	1.393 (4)
C8–C9	1.438 (5)	C17–C18	1.372 (4)
C2–C3	1.351 (5)	C18–C19	1.407 (4)
C7–C8	1.308 (4)	C19–C20	1.346 (5)
C5–C4	1.389 (5)	C20–C21	1.369 (5)
C5–C6	1.367 (5)	C21–C22	1.381 (4)
C5–C11	1.498 (4)	C22–C17	1.360 (4)
N1–Mn–N2	90.92 (15)	C5–C6–C7	125.6 (4)
N1–Mn–N2'	89.08 (15)	N2–C9–C8	108.8 (3)
N1–Mn–O1	87.97 (8)	N2–C9–C10'	127.3 (4)
N1–Mn–O1'	92.03 (8)	C8–C9–C10'	123.9 (4)
N2–Mn–O1	92.25 (8)	C1–C2–C3	106.9 (3)
N2–Mn–O1'	87.75 (8)	C2–C3–C4	107.6 (3)
Mn–O1–C23	127.2 (2)	C6–C7–C8	109.0 (3)
Mn–N1–C1	128.8 (3)	C7–C8–C9	107.6 (3)
Mn–N1–C4	127.0 (3)	C4–C5–C6	124.1 (4)
Mn–N2–C6	124.1 (3)	C4–C5–C11	118.4 (4)
Mn–N2–C9	126.7 (3)	C6–C5–C11	117.5 (4)
C1–N1–C4	103.9 (4)	C1–C10–C9'	123.4 (3)
C6–N2–C9	109.2 (4)	C1–C10–C17	118.5 (3)
N1–C1–C2	111.9 (4)	C9'–C10–C17	118.0 (4)
N1–C1–C10	124.4 (4)	C5–C11–C12	121.1 (3)
C2–C1–C10	123.7 (3)	C5–C11–C16	120.4 (3)
N1–C4–C3	109.8 (4)	C12–C11–C16	118.5 (3)
N1–C4–C5	125.0 (4)	C10–C17–C18	120.6 (3)
C3–C4–C5	125.2 (4)	C10–C17–C22	120.6 (3)
N2–C6–C5	128.8 (4)	C18–C17–C22	118.8 (3)
N2–C6–C7	105.4 (4)		

^a The esd's are calculated including the correlation terms derived from the inverted least-squares matrix. ^b Distances and bond angles are uncorrected for thermal motion. ^c Primed atoms are related to input atoms by the inversion center at (0, 0, 0).

No conclusions should be drawn from the apparent deviations in bond lengths within the porphyrin core due to the large anisotropic thermal parameters and apparent bond length differences in what are expected to be chemically equivalent bonds.

Discussion

The oxidation of $\text{Mn}^{\text{III}}\text{TPP}(\text{OAc})$ in basic methanol using either sodium hypochlorite or iodosylbenzene as the oxidant yields $\text{Mn}^{\text{IV}}\text{TPP}(\text{OCH}_3)_2$ (**1**) as the isolated product. We find that the reaction of iodosylbenzene with $\text{Mn}^{\text{II}}\text{TPP}$ made in situ in methanol also yields $\text{MnTPP}(\text{OCH}_3)_2$ as the isolated product, in contrast to the reported synthesis of the complex $\text{O}=\text{Mn}^{\text{IV}}\text{TPP}$ under similar conditions.⁶ A reevaluation of the infrared labeling study and other data used to identify

(26) Johnson, C. K. Report ORNL-3794; Oak Ridge National Laboratory; Oak Ridge, TN, 1965.

$O=Mn^{IV}TPP$ indicates no compelling evidence for the isolation of this species (see Attempted Synthesis of $O=MnTPP$ under Results).

The determination of the ground electronic state in $MnTPP(OCH_3)_2$ is needed to understand its properties. The one-electron oxidation of manganese(III) porphyrin complexes can occur either at the metal ion to give a manganese(IV) porphyrin complex or at the porphyrin ligand to give a manganese(III) porphyrin π cation radical. Goff, Reed, and co-workers²⁰ recently reported that the one-electron oxidation of $Mn^{III}(TPP)Cl$ occurs at the ligand to give the complex $[Mn(TPP)Cl]ClO_4$. The assignment of a Mn(III) porphyrin π -cation-radical ground electronic state was based upon its strong infrared absorption near 1280 cm^{-1} , which appears to be characteristic of tetraphenylporphyrin π cation radicals. The lack of strong IR absorptions in this region for **1** indicates that ligand-centered oxidation has not occurred. Hence, the oxidation was metal centered to give a manganese(IV) porphyrin complex. The magnetic susceptibility of **1**, $\mu_{\text{eff}} = 3.9\ \mu_B$, excludes a low-spin $S = 1/2$ Mn(IV) ion. Therefore, $MnTPP(OCH_3)_2$ has a d^3 high-spin Mn(IV) porphyrin ground electronic state.

The axial Mn–O bond lengths of $1.839(2)\ \text{\AA}$ in $Mn^{IV}TPP(OCH_3)_2$ are consistent with a Mn(IV) center as they are comparable to the $1.853(2)\ \text{\AA}$ Mn–O bond lengths in six-coordinate *trans*-bis(pyridyl)bis(3,5-di-*tert*-butylcatecholato)manganese(IV).²⁷ Further confirmation of a Mn(IV) ion is provided by noting that six-coordinate Mn(IV) and Ge(IV) complexes are known to exhibit nearly identical bond lengths (six-coordinate Mn(IV) and Ge(IV) have identical ionic radii of $0.53\ \text{\AA}$ and identical covalent radii of $0.67\ \text{\AA}$).²⁸ Hence, Mn(IV) and Ge(IV) porphyrins should exhibit very similar structures. This is the case. The crystal and molecular structure of dimethoxy(porphinato)germanium(IV) has been determined.²⁹ The average M–N bond distances in both $Mn^{IV}TPP(OCH_3)_2$ and $Ge^{IV}(\text{porphinato})(OCH_3)_2$ are the same ($2.015\ \text{\AA}$), and the axial metal–methoxide distances (Mn–O = $1.839(2)\ \text{\AA}$, Ge–O = $1.822(1)\ \text{\AA}$) are almost identical. The similarity of these distances verifies the presence of tetravalent ions in both complexes.

The only other Mn(IV) porphyrin complex crystallographically characterized to date is the dimeric complex $[N_3Mn^{IV}TPP]_2O$.⁴ The antiferromagnetic interaction of the two Mn(IV) centers in this dimer precludes the rigorous differentiation between high-spin and low-spin Mn(IV) centers by magnetic susceptibility measurements. However, the averages of the equatorial Mn–N_{pyrrole} distances in this complex and in $MnTPP(OCH_3)_2$ are identical. The average of the axial bond lengths in $[N_3MnTPP]_2O$ ($1.882\ \text{\AA}$) is also very close to the axial distance in $Mn^{IV}TPP(OCH_3)_2$ ($1.839(2)\ \text{\AA}$). This suggests that the dimeric complex also contains high-spin d^3 Mn(IV) centers.

Magnetic susceptibility measurements on **1**, both in solution and in the solid state, gave $\mu_{\text{eff}} = 3.9\ \mu_B$ at $25\ ^\circ\text{C}$, indicating no evidence of spin changes upon dissolution of the complex. Variable-temperature magnetic susceptibility measurements on **1** from 5 to 300 K showed Curie–Weiss behavior with $\Theta = -0.5\ \text{K}$ and $\mu_{\text{eff}} = 3.91 \pm 0.02\ \mu_B$. The μ_{eff} value is typical of Mn(IV) ions,³⁰ and a small Weiss constant is expected for a monomeric d^3 ion.^{30a} The slight increase in μ_{eff} over the expected spin-only value for a d^3 ion ($\mu_{\text{so}} = 3.87\ \mu_B$)^{30a} may

be due to the presence of trace amounts of Mn(III) complexes in the sample. The insignificant variation of μ_{eff} from 5 to 300 K indicates no evidence of temperature-dependent spin changes. Temperature-dependent intramolecular electron transfer has been observed in $[NiTPP]ClO_4$, where the ground electronic state is believed to convert from a Ni(III) porphyrin to a Ni(II) porphyrin π cation radical upon cooling.³¹

The visible spectrum of $Mn^{IV}TPP(OCH_3)_2$ is quite distinct from the visible spectra exhibited by trivalent and divalent manganese porphyrin complexes (Figure 1). The visible spectrum is also very different from the complicated spectra exhibited by the formally isoelectronic d^3 Cr(III) porphyrins. In Cr(III) porphyrin complexes, it is believed that the small energy separation between the porphyrin-centered π^* orbitals and the metal-centered d_{xz} and d_{yz} orbitals causes substantial mixing of these orbitals to occur.³² The higher effective charge on the d^3 ion in $Mn^{IV}TPP(OCH_3)_2$ should substantially lower the d_{xz} and d_{yz} orbital energies and cause the mixing with the ligand π^* orbitals to be reduced. Hence, Mn(IV) and Cr(III) porphyrins are expected to exhibit spectroscopic differences.

Manganese porphyrin complexes with oxygen-containing ligands can be expected to be key intermediates in the reported oxygen and hydrogen peroxide evolving reactions involving high-valent manganese porphyrin complexes.³ $Mn^{IV}TPP(OCH_3)_2$ represents a model for dihydroxymanganese(IV) porphyrin complexes that could exist in these systems. A dihydroxymanganese(IV) porphyrin complex can be expected to exhibit the same electronic state as $Mn^{IV}TPP(OCH_3)_2$ due to the similarity of their axial ligands. The low magnetic moments ($\mu_{\text{eff}} \sim 2\ \mu_B$)³³ reported for the water-soluble porphyrins oxidized under basic conditions indicate monomeric dihydroxymanganese(IV) porphyrin complexes are not the predominant species present.

Manganese porphyrin complexes have been reported to catalyze the oxidation of alcohols to aldehydes under basic conditions.^{2h,j} Our studies suggest that dialkoxymanganese(IV) porphyrin complexes are likely to be present under these conditions. The study of the pH-dependent reduction of dialkoxymanganese(IV) porphyrin complexes should aid in understanding the mechanism of these reactions.

Several systems utilizing manganese porphyrins as catalysts have been reported to be able to oxidize alkanes at room temperature.^{2a-c,e-b} The active intermediates in these reactions have been hypothesized to be $O=Mn^V$ porphyrin species.^{2g} However, the reactivity of monomeric Mn(IV) porphyrins toward hydrocarbons has not been studied. Further characterization and study of the reactivity of monomeric Mn(IV) porphyrins will be required to determine whether they are present in these systems and whether they are also capable of the observed hydrocarbon oxidations. Further studies on the synthesis of high-valent manganese porphyrin complexes and their potential as catalysts for hydrocarbon activation and water oxidation are in progress in our laboratories.

Acknowledgment. Support of this work by the National Science Foundation (Grant No. CHE-7909730) and by the donors of the Petroleum Research Fund, administered by the American Chemical Society, is acknowledged. We acknowledge NSF Grant No. CHE-8026039 for purchase of the SQUID susceptometer.

Registry No. $MnTPP(OCH_3)_2$, 83095-80-1; $Mn^{III}TPP(OAc)$, 58356-65-3; $Mn^{II}TPP$, 31004-82-7; $Mn^{II}TPP \cdot 2CH_3OH$, 83095-81-2; $MnTPP(OCH_3)_2 \cdot 1/4CH_3OH$, 83095-82-3; deuterium, 7782-39-0.

Supplementary Material Available: Infrared spectra of $MnTPP$ -

(27) Lynch, M. W.; Hendrickson, D. N.; Fitzgerald, B. J.; Pierpont, C. G. *J. Am. Chem. Soc.* **1981**, *103*, 3961.

(28) Shannon, R. D. *Acta Crystallogr., Sect. A* **1976**, *A32*, 751.

(29) Mavridis, A.; Tulinsky, A. *Inorg. Chem.* **1976**, *15*, 2723.

(30) (a) Figgis, B. N.; Lewis, J. *Prog. Inorg. Chem.* **1964**, *6*, 37. (b) König, E.; König, G. In "Landolt-Börnstein. Numerical Data and Functional Relationships in Science and Technology"; Springer-Verlag: New York, 1981; New Series, Group II, Vol. 11, Suppl. 3, p. 10.

(31) Johnson, E. C.; Niemi, T.; Dolphin, D. *Can. J. Chem.* **1978**, *56*, 1381.

(32) Gouterman, M.; Hanson, L. K.; Khalil, G.-E.; Leenstra, W. R. *J. Chem. Phys.* **1975**, *62*, 2343.

(33) (a) Harriman, A.; Porter, G. *J. Chem. Soc., Faraday Trans. 2* **1979**, *75*, 1532. (b) Loach, P. A.; Calvin, M. *Biochemistry* **1963**, *2*, 361.

(OCH₃)₂, MnTPP(OCD₃)₂, and C₆H₅I (Figure S1), variable-temperature magnetic susceptibility data (Table SI) and details of calculations, crystallographic data including anisotropic thermal parameters for non-hydrogen atoms (Table SII), observed and calculated

structure factor amplitudes (Table SIII), final hydrogen atom positional and thermal parameters (Table SIV), least-squares planes (Table SV), and intermolecular contacts (Table SVI) (22 pages). Ordering information is given on any current masthead page.

Contribution from the Lehrstuhl für Anorganische Chemie I der Ruhr-Universität, D-4630 Bochum, West Germany, and the Anorganisch-Chemisches Institut der Universität Heidelberg, D-6900 Heidelberg, West Germany

1,4,7-Triazacyclononane-*N,N',N''*-triacetate (TCTA), a Hexadentate Ligand for Divalent and Trivalent Metal Ions. Crystal Structures of [Cr^{III}(TCTA)], [Fe^{III}(TCTA)], and Na[Cu^{II}(TCTA)]·2NaBr·8H₂O

KARL WIEGHARDT,*^{1a} URSULA BOSSEK,^{1a} PHALGUNI CHAUDHURI,^{1a} WILLY HERRMANN,^{1a} BERNHARD C. MENKE,^{1a} and JOHANNES WEISS*^{1b}

Received April 28, 1982

Monomeric complexes of di- and trivalent metal ions containing the potentially hexadentate ligand 1,4,7-triazacyclononane-*N,N',N''*-triacetate (TCTA) have been synthesized: [M^{III}(TCTA)], M = Al, Cr, Mn, Fe, Co, and [M^{II}(TCTA)]⁻, M = Mn, Fe, Co, Ni, Cu. The crystal structures of [Cr^{III}(TCTA)] (1), [Fe^{III}(TCTA)] (2), and Na[Cu^{II}(TCTA)]·2NaBr·8H₂O (3) have been determined by single-crystal X-ray diffraction. Crystals of 1 were monoclinic with space group C_{2h}²-P2₁/n (*a* = 8.825 (9) Å, *b* = 13.458 (7) Å, *c* = 11.913 (12) Å, β = 106.09 (10)°, *Z* = 4, *V* = 1360 Å³). The structure consists of neutral complexes of [Cr(TCTA)] with a chromium(III) ion in a distorted-octahedral environment of a facial N₃O₃ donor set. Crystals of 2 were rhombohedral with space group C_{3v}²-R3c (*a* = 13.577 (3) Å, *Z* = 6, *V* = 2117 Å³). The neutral molecules of [Fe^{III}(TCTA)] have crystallographically imposed C₃ symmetry. The iron(III) ions are in a distorted-pseudoprismatic environment. Crystals of 3 were triclinic with space group C₁¹-P1̄ (*a* = 9.156 (1) Å, *b* = 11.679 (3) Å, *c* = 14.131 (2) Å, α = 104.14 (2)°, β = 103.81 (1)°, γ = 102.74 (2)°, *Z* = 2, *V* = 1388 Å³). The structure consists of two monoanions of [Cu^{II}(TCTA)]⁻, sodium and uncomplexed bromide ions, and molecules of water of crystallization. The Cu(II) ions are in a highly distorted pseudoprismatic environment of N₃O₃ donor atoms. The visible absorption spectra, magnetic moments, and pertinent infrared data are described. Formal reduction potentials for the couples [Cr(TCTA)]^{0/-}, [Mn(TCTA)]^{0/-}, [Fe(TCTA)]^{0/-}, [Co(TCTA)]^{0/-}, and [Ni(TCTA)]^{0/-} vs. the normal hydrogen electrode have been determined from their reversible cyclic voltammograms (-1.17, +0.80, +0.195, 0.00, and +1.16 V, respectively).

Introduction

Syntheses for tetraaza macrocycles with four N-bonded acetate groups have recently been published.²⁻⁴ The stabilities of metal complexes containing these EDTA analogues appear to be large and in some cases even larger than are observed for the corresponding EDTA complexes.²⁻⁴ Kaden et al.³ have proposed that these potentially octadentate ligands coordinate metal ions such as Cu(II) and Ni(II) in a pseudooctahedral fashion where only two nitrogen atoms of the ligand and two oxygens of the carboxylate groups are bound to the metal centers.

In view of the propensity of most divalent and trivalent transition-metal ions for the coordination number 6 we have synthesized the ligand 1,4,7-triazacyclononane-*N,N',N''*-triacetate. This ligand is ideally suited to be wrapped around metal ions. It is to be expected that the first and second coordination spheres of such complexes should change only slightly in some instances when the oxidation state of the metal center is increased or decreased by 1 unit via outer-sphere electron-transfer reactions. Therefore, we believe that a series of such complexes is ideally suited for delineating factors governing the electron-transfer rates of outer-sphere reactions in homogeneous solutions. We report here the preparation and structural characterization of these complexes containing the ligand.

Experimental Section

Preparation of the Ligand. The starting compound 1,4,7-triazacyclononane trihydrobromide was prepared according to a modified method⁵ described by Atkins and co-workers.⁶ Aqueous solutions

containing the ligand 1,4,7-triazacyclononane-*N,N',N''*-triacetate (TCTA) were prepared by following procedures reported for the syntheses of similar tetraaza tetraacetate macrocycles.²⁻⁴ To a solution of 37.1 g of 1,4,7-triazacyclononane trihydrobromide (0.1 mol) and 12.0 g of NaOH (0.3 mol) in 35 mL of water was added with stirring at 20 °C a second solution containing 47.2 g of bromoacetic acid (0.3 mol) and 12.0 g of NaOH in 100 mL of water. The temperature was raised to 80 °C, and 12.0 g of NaOH dissolved in 65 mL of water was added dropwise. The temperature was maintained at 80 °C for 1 h, after which time the reaction was completed. The pH of the solution was adjusted to 7 with concentrated HBr. Attempts to isolate a crystalline sodium salt of the ligand or the uncomplexed acid from such solutions at pH 12, 7, 2.5, and 1 have failed. Portions of the above solution were subsequently used for the preparation of metal complexes ([ligand] ≈ 0.66 M, [Br⁻] ≈ 2.6 M).

Preparation of Complexes. **[Al(TCTA)].** To 20 mL of the above solution containing the ligand TCTA was added at 60 °C 2.0 g of AlCl₃·6H₂O dissolved in 30 mL of water. The pH of the solution (~0.7) was slowly raised to 7 with 0.5 M NaOH. When the solution cooled, colorless, needle-shaped crystals precipitated, which could be recrystallized from hot water. Anal. Calcd for [AlCl₂H₁₈N₃O₆]: C, 44.04; H, 5.54; N, 12.84. Found: C, 43.8; H, 5.3; N, 12.6.

[VO(TCTAH)]·H₂O. To 20 mL of the ligand solution was added a solution of 2.6 g of VO(SO₄)·5H₂O dissolved in 40 mL of water, and the pH of the resulting solution was adjusted to 1.5. When the solution stood for 2 days at 20 °C, blue-violet crystals precipitated. These were filtered off, washed with ethanol and ether, and air-dried. Anal. Calcd for [C₁₂H₁₉N₃O₇V]·H₂O: C, 37.31; H, 5.48; N, 10.88; V, 13.19. Found: C, 37.2; H, 5.4; N, 11.0; V, 13.4.

[Cr(TCTA)]. To 20 mL of the ligand solution was added 5.4 g of Cr(ClO₄)₃·6H₂O dissolved in 20 mL of water. The solution was refluxed until a clear red solution was obtained. The pH was adjusted to 7 from time to time by adding 0.5 M NaOH. When the solution

(1) (a) Ruhr-Universität. (b) Universität Heidelberg.
 (2) Stetter, H.; Frank, W. *Angew. Chem.* 1976, 88, 760.
 (3) Häflinger, H.; Kaden, I. A. *Helv. Chim. Acta* 1979, 62, 683.
 (4) Desreux, J. F. *Inorg. Chem.* 1980, 19, 1319.

(5) Wiegardt, K.; Schmidt, W.; Nuber, B.; Weiss, J. *Chem. Ber.* 1979, 112, 2220.
 (6) Atkins, T. J.; Richman, J. E.; Oettle, W. F. *Org. Synth.* 1978, 58, 86.